

Accurate Transport Modeling with 2D Dopant Profile Effect in $L_{\text{eff}} \sim 20$ nm MOSFETs via Inverse Modeling

†Takuji Tanaka, Hiroyuki Kanata, Yukio Tagawa, Shigeo Satoh, and Toshihiro Sugii
FUJITSU Limited

50 Fuchigami, Akiruno, Tokyo 197-0833 Japan

Tel: +81-42-532-1253, Fax: +81-42-532-2514, E-mail: †tanaka.takuji@jpf.fujitsu.com

ABSTRACT

To accurately consider 2D dopant profile effect, we have studied transport modeling by comparing nMOSFETs with indium or boron pocket implant. Our inverse modeling has successfully extracted their features of dopant profiles and DIBL effects. It has enabled us to evaluate that the generalized hydrodynamic model is highly reliable even in smaller MOSFETs down to $L_{\text{eff}} \sim 20$ nm.

INTRODUCTION

To accurately calculate drain conductance ($g_{ds} \equiv \partial I_{ds} / \partial V_d$), a key parameter in analog circuits, we must separate two dimensional (2D) profile effects (i.e. drain induced barrier lowering, DIBL) from transport modeling issues (i.e. non-equilibrium transport effects) since both affects g_{ds} . It is known that correct device structure is needed to be known for transport modeling, where inverse modeling (IM) method is powerful to extract dopant profile [1, 2].

In this paper, we study transport modeling by comparing nMOSFETs with indium or boron pocket implant to examine 2D dopant profile effects. To extract the 2D profile, we use our IM method which properly includes short channel effect. We report the generalized hydrodynamic model (GHDM) [3] well describes current of MOSFETs with a wide range of applied voltages, channel profiles, and device sizes down to $L_{\text{eff}} \sim 20$ nm.

EXTRACTION OF 2D DOPANT PROFILE

We have extracted 2D dopant profile by our inverse modeling method [4] which takes L_{gate} dependence of short channel effect (V_{th} rollofs, S factor rollups, DIBL, and back bias factors) into account. Note those targeted device parameters are independent of transport modeling issues (i.e. high field transport effects, non-equilibrium transport effects). Since this step is free from error of the transport modeling, the extracted 2D dopant profile will be basis of the reliable transport modeling in the next section.

The flowchart is shown in Fig. 1(a). The main objective of the flow is to extract a consistent profile among different L_{gate} 's. A faster convergence is realized by the feedbacked flow which includes targeted devices step by step from longer

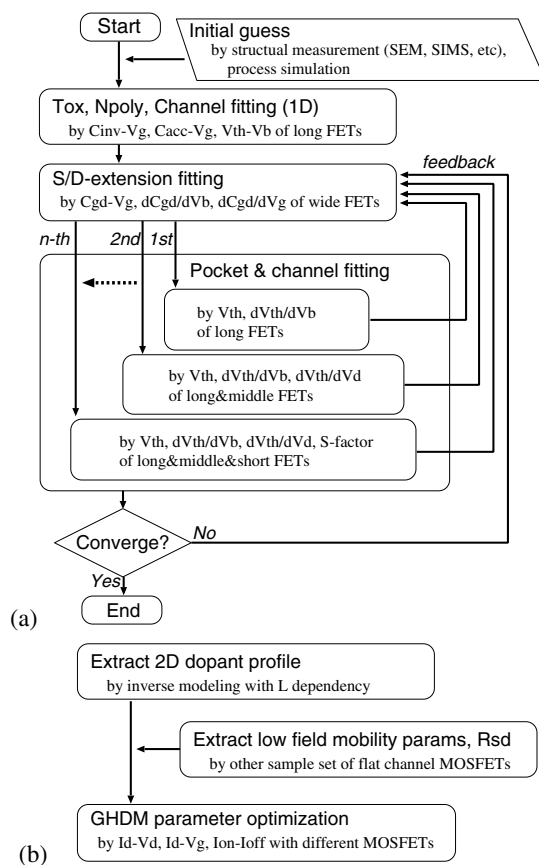


Fig. 1. Procedure of (a) extraction of 2D dopant profiles and (b) optimization of transport model parameters. Note the extraction of the dopant profiles is free from error of the transport modeling.

to shorter L_{gate} . Ten samples of L_{eff} from 2 μm to ~ 20 nm are used for the target.

Assumed dopant profile is a linear combination of functions:

$$N(x, y) = \frac{N_0}{2} e^{-\left|\frac{x-x_0}{x_d}\right|^a} \left(\operatorname{erfc} \left\{ \frac{y-y_0}{y_d} \right\} - \operatorname{erfc} \left\{ \frac{y-y_1}{y_d} \right\} \right),$$

where x is the coordinate perpendicular to the channel, y is the coordinate parallel to the channel, and $N_0, a, x_0, x_d, y_0, y_1,$

TABLE I
MEASURED AND ANALYZED SAMPLE OF NMOSFETS WITH DIFFERENT
POCKET DOSE CONDITION.

ID	pocket dose dopant	amount	ID	pocket dose dopant	amount
#In-L	Indium	low	#B-L	Boron	low
#In-H	Indium	high	#B-H	Boron	high

and y_d are parameters. The channel profile consists of three functions for each (left/right) side of pocket dopant and three functions for V_{th} control and well dopant. Function parameters keep constant and only L_{gate} is changed for different L_{gate} devices. The assumption of the profile takes an advantage to analyze continuous change of the short channel effects.

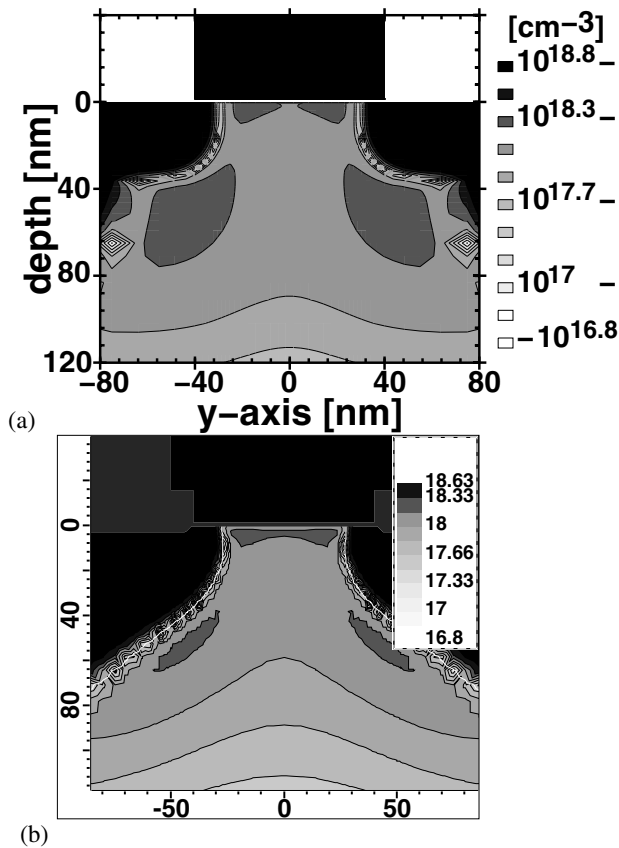


Fig. 2. Comparison of 2D dopant profiles of a MOSFET between (a) that extracted by our inverse modeling and (b) that calculated by the process simulator *TSUPREM4*.

To confirm accuracy of IM we have compared profile of a test sample by IM to that calculated by a process simulator *TSUPREM4*. As shown in Fig. 2, they show very good agreement.

We prepared samples with different pocket dose condition as listed in Tab. I. They actually have different DIBL and back bias effects with L_{gate} dependencies as shown in Fig. 3. Our results of IM are shown in Figs. 3 and 4: V_{th} rolloffs reproduced by IM and extracted dopant profiles by IM. The smaller DIBL and the larger back bias effect are measured

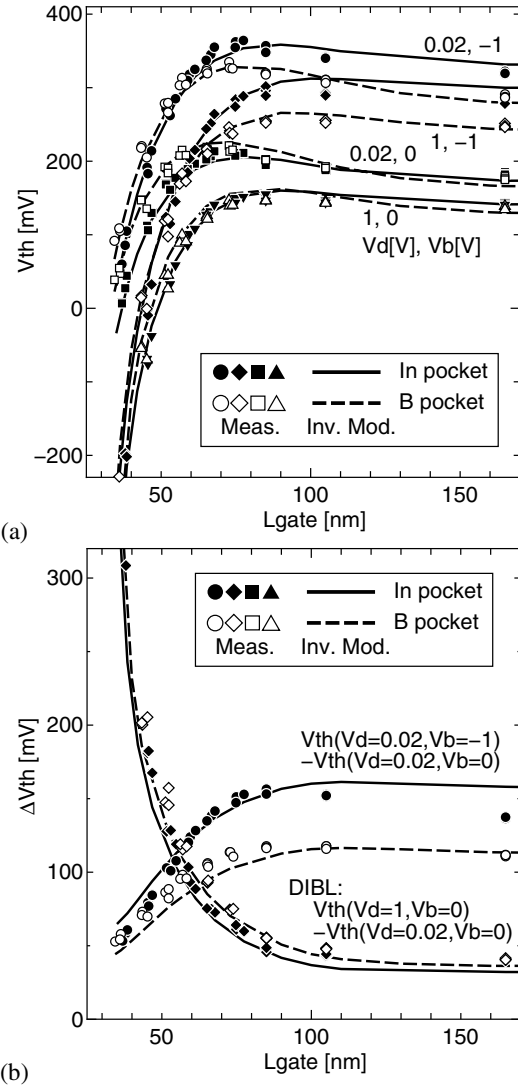


Fig. 3. (a) V_{th} and (b) ΔV_{th} dependence on L_{gate} of indium (#In-H) and boron (#B-H) samples comparing measurement and calculation reproduced by inverse modeling. The extracted 2D dopant profiles by the inverse modeling are shown in Fig. 4.

in #In-H compared to that in #B-H. Those properties are well reproduced by IM (Fig. 3). The difference is reasonably explained by the extracted 2D channel profiles of retrograde one in #In-H and pile-uped one in #B-H (Fig. 4).

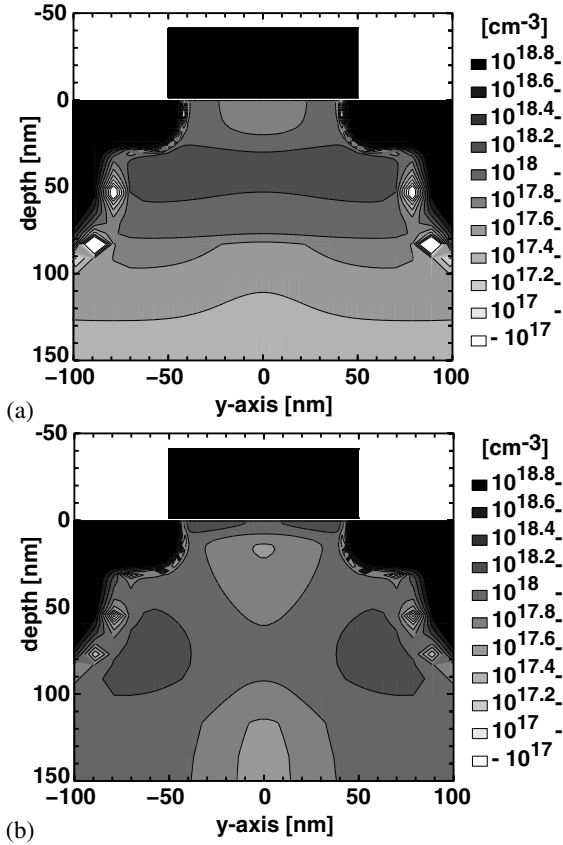


Fig. 4. Extracted 2D dopant profiles of (a) #In-H and (b) #B-H by inverse modeling with $L_{gate} = 100$ nm. Reasonable retrograde profile in #In-H and pile-up profile in #B-H are clearly found. The calculated $V_{th-L_{gate}}$ and $\Delta V_{th-L_{gate}}$ relation with those profiles is shown in Fig. 3.

TRANSPORT MODELING

The flowchart of transport modeling is shown in Fig. 1(b). Prior to non-equilibrium transport modeling, we optimized the model parameters related to equilibrium transport effects: low field inversion layer mobility and parasitic resistance.

Our calculation has done by a device simulator *GALENE3* [3] revised by us. We have adopted a low field inversion layer mobility model by Darwish *et al.* [5] and the model parameters are optimized to our SiON gate insulator film with wide range of channel density variation ($1 \times 10^{16} \text{ cm}^{-3} < N_A < 1 \times 10^{19} \text{ cm}^{-3}$). Hänsch model [6,7] is applied for quantum effects.

For the transport modeling, we have applied the generalized hydrodynamic model (GHDM) [3] which takes nonparabolic band structure into account. The basic transport equations are:

$$\begin{aligned}
 \epsilon \Delta \Psi &= -q(p - n + N_D - N_A) \\
 \nabla J &= qR \\
 J &= -\frac{q}{m^*} \left\{ \tau_i^* q n \nabla \Psi - \tau_i k T^* \nabla n - f_{td} \tau_i n \nabla k T^* \right\} \\
 \nabla S &= -J \nabla \Psi - \frac{3}{2} k \left\{ n \tau_w^{*-1} (T^* - T_{eq}) + T^* R \right\} \\
 S &= -\frac{5}{2q} k T^* \tau_s^* \tau_i^{*-1} \left\{ J + f_{hf} \frac{q}{m^*} \tau_i n \nabla k T^* \right\}.
 \end{aligned}$$

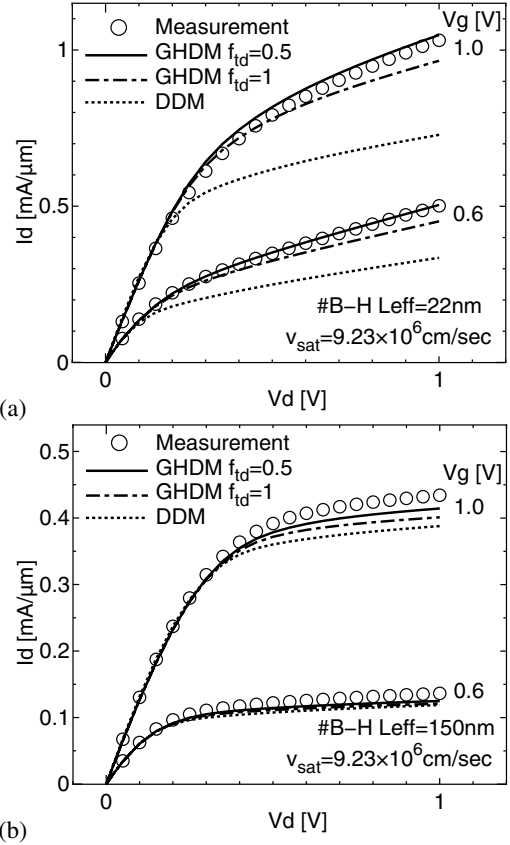


Fig. 5. Transport model dependency on I_d-V_d of MOSFETs with (a) $L_{eff} = 22$ nm and (b) 150 nm.

All symbols have their usual meaning and are defined in [3]. $f_{td} = 1$ and $f_{hf} = 1$ is related to a fourth order moment of the Boltzmann transport equations.

Reference 8 has reported that the original GHDM parameters $f_{td} = f_{hf} = 1$ gives much larger velocity overshoot at the drain edge and smaller value of f_{td} or f_{hf} gives better agreement with a Monte Carlo carrier transport modeling. Figure 5 compares I_d-V_d curves among transport models. We see in the shortest $L_{gate} = 22$ nm the conventional drift-diffusion model (DDM) is no longer valid and GHDM with a modification of $(f_{td}, f_{hf}) = (0.5, 1)$ gives the best fit. This result is consistent with Ref. [8].

Figure 6 shows I_d-V_d at $L_{gate} = 22$ nm calculated by GHDM($f_{td} = 0.5$). g_{ds} well agrees between measurement and calculation for each device with different DIBL. Figure 7 shows $I_{on}-I_{off}$ calculated by GHDM($f_{td} = 0.5$). The calculated I_d well fits the measurements within an error of 7 % in all of the different pocket dose conditions in Tab. I, device sizes, and applied voltages. In the measurement, I_{on} is larger in indium dose than in boron dose and larger in smaller dose amount between MOSFETs with the same I_{off} 's. These features have been well reproduced by our calculation not only qualitatively but also quantitatively. These results show the modified GHDM is valid with the highest accuracy even in smaller MOSFETs down to $L_{eff} \sim 20$ nm.

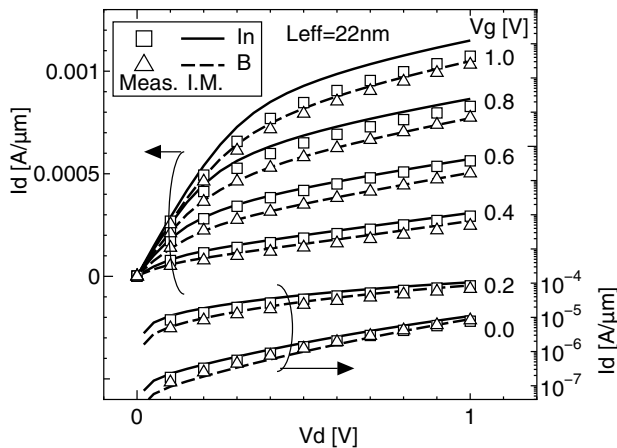


Fig. 6. I_d - V_d of $L_{\text{eff}} = 22$ nm MOSFETs in measurement and calculation comparing pocket dopant (#In-H and #B-H). The calculation is by GHDM($f_{id} = 0.5$). I_d - V_d well agrees between measurement and simulation for each sample with different DIBL effect.

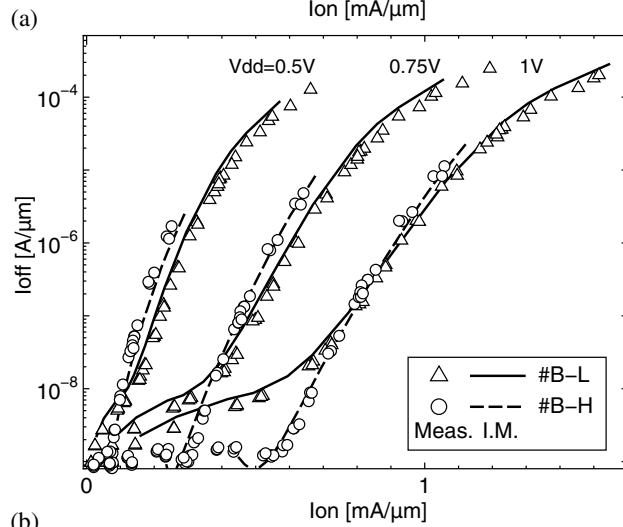
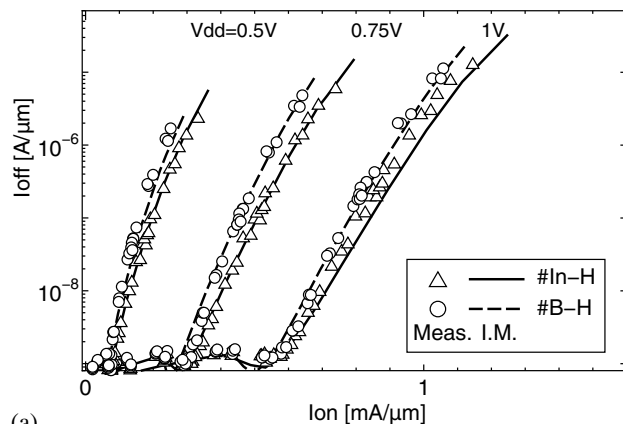


Fig. 7. I_{on} - I_{off} of measurement and calculation comparing (a) pocket dopant (In or B) and (b) pocket dose amount. The calculation is by GHDM($f_{id} = 0.5$). The calculation has well reproduced the measured feature that I_{on} is larger in indium dose than in boron dose and larger in smaller dose amount between MOSFETs with the same I_{off} 's.

CONCLUSION

Our inverse modeling has successfully extracted different features of 2D dopant profile between MOSFETs with indium and boron pocket implant and correctly evaluated DIBL effect. By our correct consideration of 2D effect, the generalized hydrodynamic model is found to be highly reliable even in smaller MOSFETs down to $L_{\text{eff}} \sim 20$ nm.

REFERENCES

- [1] D. A. Antoniadis *et al.*, "Electron velocity in sub-50-nm channel MOSFETs", International Conference on Simulation of Semiconductor Processes and Devices (SISPAD) pp.156-61, 2001.
- [2] H. Goto *et al.*, "Inverse modeling as a basis for predictive device simulation of deep submicron MOSFETs", Jpn. J. of Appl. Phys. **37** pp.5437-43, 1998.
- [3] R. Thoma *et al.*, "Hydrodynamic equations for semiconductors with nonparabolic band structure", IEEE Trans. on Elec. Devices **38** pp.1343-53, 1991.
- [4] Takuji Tanaka *et al.*, "Characterization of 2D dopant profile in $L_{\text{eff}} \sim 20$ nm MOSFETs by inverse modeling with precise $\partial C/\partial V$, $\partial V_{\text{th}}/\partial V-L$ measurement", International Electron Devices Meeting (IEDM) Tech. Digest pp.887-90, 2002.
- [5] M. N. Darwish *et al.*, "An improved electron and hole mobility for general purpose device simulation", IEEE Trans. on Elec. Devices **44** pp.1529-38, 1997.
- [6] W. Hänsch *et al.*, "Carrier transport near the Si/SiO₂ interface of a MOSFET", Solid State Electron. **32** pp.839-49, 1989.
- [7] Rafael Rios *et al.*, "Determination of ultra-thin gate oxide thickness for CMOS structures using quantum effects", International Electron Devices Meeting (IEDM) Tech. Digest pp.613-6, 1994.
- [8] B. Meinerzhagen *et al.*, "On the consistency of the hydrodynamic and the Monte Carlo models", Proceedings of International Workshop Computational Electronics (IWCE) pp.7-12, 1992.